Unravelling the postural diversity of mammals: Contribution of humeral cross-sections to palaeobiological inferences

Jordan Gônet, Jérémie Bardin, Marc Girondot, John R Hutchinson, Michel Laurin

Unravelling the postural diversity of mammals: Contribution of humeral cross-sections to palaeobiological inferences

Jordan Gônet[1]* · Jérémie Bardin[1] · Marc Girondot[2] · John R. Hutchinson[3] · Michel Laurin[1]

[1]Centre de recherche en paléontologie – Paris, UMR 7207, Sorbonne Université, Muséum national d'histoire naturelle, Centre national de la recherche scientifique, 8 rue Buffon, 75005 Paris, France

[2]Laboratoire écologie, systématique et évolution, UMR 8079, AgroParisTech, Université Paris-Saclay, Centre national de la recherche scientifique, 91405 Orsay, France

[3]Structure and Motion Laboratory, Department of Comparative Biomedical Sciences, Royal Veterinary College, AL9 7TA Hatfield, UK

*Corresponding author: jordan.gonet@edu.mnhn.fr

Keywords: Functional morphology · Humerus · Limb posture · Mammal · Microanatomy · Palaeobiology

Abstract

Mammals have an evolutionary history spanning hundreds of millions of years. Today, mammals represent one of the most diverse groups of tetrapod vertebrates. In particular, they present a great postural diversity. The humerus adopts different positions: small mammals have a “crouched” posture with a quasi-horizontal humerus, while in the largest species, the humerus is more vertical. Some monotremes have more transversely oriented humeri similar to those of reptiles. The forelimb of moles is also modified in relation to their burrowing lifestyle. This postural diversity is accompanied by an important microanatomical disparity. Indeed, the bones of the appendicular skeleton support the weight of the body and are subjected to various forces that partly shape their external and internal morphology. We show here how geometric and microanatomical parameters measured in cross-section such as the polar section modulus or the position of the medullo-cortical transition can be related to posture. Using statistical methods that take phylogeny into account, we develop a postural model from a sample of humerus cross-sections belonging to 41 species of extant mammals. Our model can be used by palaeontologists to infer the posture of extinct synapsids. As an example, we infer the posture of two emblematic taxa: *Dimetrodon natalis* and *Peratherium cuvieri*. The results of the analysis indicate a sprawling posture for *Dimetrodon* and a crouched posture for *Peratherium*. This work contributes to unravel the complex interaction between phylogeny, humeral microanatomy and geometry, body mass, lifestyle and posture in mammals.

Introduction

Mammals are a highly successful group of tetrapod vertebrates with a long evolutionary history. Their earliest stem members, i.e. the first synapsids (the term "stem mammal" is used throughout this study to refer to any taxon that is more closely related to Mammalia than to Reptilia but that does not belong to the mammalian crown group), originated in the Carboniferous, about 330 million years ago, with the emergence of the first amniotes (Didier and Laurin 2020), and have undergone several episodes of diversification ever since. The Late Carboniferous and Early Permian is dominated by eupelycosaurs. These are followed by therapsids by the middle Permian; they comprised medium-sized herbivorous and carnivorous taxa that became extinct by the end of the Triassic, except for cynodonts, which gave rise to the Mammaliaformes during the Triassic (Kemp 2005; Brocklehurst et al. 2013). It is generally thought that most Mesozoic mammals were small, nocturnal creatures with more or less burrowing habits and a generalised insectivory (Jenkins and Parrington 1976; Kielan-Jaworowska et al. 2004; Gerkema et al. 2013; but see Hu et al. 2005; Gill et al. 2014; Meng 2014; Debuysschere 2015). The K-Pg extinction event was the starting point for the Cenozoic radiation of mammals which led them to colonise the ecological niches left empty by non-avian dinosaurs (Rose 2006; but see Wilson et al. 2012). Today, mammals are extremely diverse, both taxonomically and ecologically. With over 5,000 currently recognised extant species (Upham et al. 2019), they are found all over the world, at all levels of the trophic network, on land, in the seas and in the air (Vaughan et al. 2015). They range in size from the bumblebee bat, which weighs only a few grams, to the blue whale (the largest animal on the planet), which weighs more than 100 tons, the weight of a few dozen elephants. Mammals are also particularly diverse in their posture: small mammals like rodents have a "crouched" posture, with a quasi-horizontal humerus (Jenkins 1971), while in the cursorial and graviportal taxa, such as artiodactyls and proboscideans, the humerus is more vertical (Gregory 1912). Some monotremes have more transversely oriented humeri (Pridmore 1985). The forelimb of moles is also modified in relation to their burrowing lifestyle (Lin et al. 2019).

The shape of biological structures is determined by at least three types of constraints that can be positioned at the three vertices of an abstract triangle in the framework of constructional morphology (Seilacher 1970). These are phylogenetic (heredity), structural (development), and adaptive (function) constraints. The bones of the appendicular skeleton are subject to these different constraints, especially functional constraints relative to posture. Indeed, limb bones support the weight of the body and are affected by various forces that partly

shape their external and internal morphology. While many studies have already identified the link between lifestyle (from aquatic to terrestrial) and bone microanatomy, including using multivariate quantitative methods that take phylogeny into account (Germain and Laurin 2005; Kriloff et al. 2008; Canoville and Laurin 2009, 2010; Laurin et al. 2011; Quemeneur et al. 2013; Amson et al. 2014; Ibrahim et al. 2014; Nakajima et al. 2014; Cooper et al. 2016; Houssaye et al. 2016a; Klein et al. 2016; Houssaye and Botton-Divet 2018; Kilbourne and Hutchinson 2019; Canoville et al. 2021; Fabbri et al. 2022), fewer have attempted to link the geometric and microanatomical properties of limb bones to posture (Houssaye et al. 2016b; Bishop et al. 2018a, 2018b, 2018c; Plasse et al. 2019; Main et al. 2021; Wagstaffe et al. 2022).

Although it is accepted that mammals, like reptiles such as dinosaurs and pseudosuchians (Hutchinson 2006), experienced a postural transition from approximately transversely-oriented to more parasagittally-oriented limbs, the timing of this transition has been widely debated without reaching a consensus. Some authors (Jenkins 1973; Pridmore 1985; Sereno 2006) have argued that early mammals had already acquired a parasagittal limb posture and gait by the Late Triassic/Early Jurassic, while others (Gambaryan and Kielan-Jaworowska 1997; Kielan-Jaworowska and Hurum 2006) favoured the hypothesis of a later acquisition in early therians. Even today, posture in mammals and in older stem taxa such as *Dimetrodon*, raises many questions that triggered numerous studies that enrich our knowledge of the evolution of locomotion in mammals (Abbott 2019; Regnault et al. 2020; Jones et al. 2021; Brocklehurst et al. 2022).

Our study is a logical extension of these works. Using generalised least squares, we investigate the relationship between humeral posture and geometric and microanatomical data collected from humeral bone cross-sections belonging to 41 extant mammalian species, while taking phylogeny into account. Body mass and lifestyle were also included in our models as both are known to be related to posture and/or bone microanatomy, e.g. large taxa tend to have greater bone compactness and more upright limbs (Biewener 1989b; Houssaye et al. 2016b); fossorial talpids have greater extension of the medullo-cortical transition compared to terrestrial talpids (Meier et al. 2013). We use the collected data to generate a phylogenetically informed postural inference model capable of generating postural predictions in extinct taxa. We apply the model to two taxa: *Dimetrodon natalis* (a small *Dimetrodon* species) and *Peratherium cuvieri* ("Cuvier's Sarigue"). While *Dimetrodon* is a stem mammal, *Peratherium* is a putative marsupialiform. *Dimetrodon* and *Peratherium* lived in the Early Permian and Late Eocene, respectively, well before and well after the Mesozoic postural transition in mammals. The

posture of *Dimetrodon* has been extensively studied since its discovery in the second half of the 19th century. The recent interpretation indicates a more or less sprawling posture. In comparison, *Peratherium* has been the subject of less work, but its younger geological age and general anatomy are compatible with a more crouched posture. These two taxa are therefore perfect candidates to test our method.

Materials and Methods

Biological sample

To train our statistical model, we compiled a set of geometric and microanatomical data collected on humeral mid-diaphyseal cross-sections from a large number of mammalian taxa with a known posture. The dataset included 43 individuals from 41 extant species (Table 1; Online Resource 1). We built our dataset to be as taxonomically exhaustive as possible and to maximise coverage of the postural diversity of Mammalia. We used our postural models to infer the posture of two extinct taxa of interest: the Early Permian stem mammal *Dimetrodon natalis* (IPBSH-4) and the Late Eocene herpetotheriid *Peratherium cuvieri* (MNHN-F-GY679b); see Online Resource 1.

Postural definitions

Most non-flying mammals are obligate quadrupeds, that is, they move exclusively on four limbs (Vaughan et al. 2015). A few taxa, especially among rodents, marsupials and primates, are known to be facultatively bipedal or quadrupedal, meaning that they alternate between bipedalism and quadrupedalism (D'Août et al. 2004; Russo and Kirk 2017). Some pangolins (*Smutsia temminckii*) are also able to move on their hind limbs for some distance (Pietersen et al. 2020). Obligate bipedalism is restricted to humans (Niemitz 2010).

Yet, mammals show great diversity in limb posture, especially regarding the humerus (Fig. 1). During normal walking, the specialised "erect" (or upright) forelimb posture of mammals exhibits fairly low humeral abduction (less than 10 degrees to the parasagittal plane; Jenkins 1971). The humerus is oblique with the elbow always functioning below the shoulder joint between approximately 30 and 75 degrees from the horizontal. Erect limbs are found in "hoofed" mammals such as artiodactyls and proboscideans (Gregory 1912), in carnivorans (Blob 2000) and in cursorial and graviportal mammals in general (Gregory 1912; Jenkins 1971; but see Stein and Casinos 1997; Carrano 1999). Taxa with more generalised locomotor adaptations, such as rodents, have a so-called "crouched" posture (Jenkins 1971). The humerus

Table 1 List of the mammalian taxa included in this study. Taxa are presented in alphabetical order. Body mass is rounded to the nearest gram. *Data collected on https://www.morphosource.org. Abbreviations: Aq, semi-aquatic; Ar, arboreal; C, crouched; E, erect; Fo, fossorial; M, modified; S, sprawling; Te, terrestrial. Institutional abbreviations: IPBSH/STIPB, Steinmann-Institut, Universität Bonn, Germany; MNHN, Muséum national d'Histoire naturelle, Paris, France; NHMUK, Natural History Museum, London, United Kingdom; UFGK, Ur- und Frühgeschichte Köln, Cologne, Germany; UMZC, Cambridge University Museum of Zoology, Cambridge, United Kingdom

Taxon			Collection number	Humeral posture	Lifestyle	Body mass (g)
Afrosoricida	Chrysochloridae	*Chrysochloris asiatica*	MNHN-ZM-MO-1991-626	C	Fo	37
Artiodactyla	Bovidae	*Cephalophus silvicultor*	NHMUK ZD 1961.8.9.80-1	E	Te	62,007
		Rupicapra rupicapra	STIPB M1639	E	Te	35,383
		Syncerus caffer	NHMUK ZD 1874.11.2.4	E	Te	646,333
	Cervidae	*Alces americanus*	UMZC H.17,691	E	Te	368,500
		Cervus elaphus	MNHN unnumbered specimen	E	Te	160,167
		Rangifer tarandus	STIPB M47	E	Te	101,250
	Suidae	*Sus scrofa*	MNHN unnumbered specimen	E	Te	135,000
		Sus scrofa	STIPB M56	E	Te	135,000
Carnivora	Canidae	*Vulpes vulpes*	STIPB M12	E	Te	4,580
	Felidae	*Felis silvestris*	UFGK unnumbered specimen	E	Te	5,037
		Panthera leo	MNHN-ZM-AC-1912-398	E	Te	149,062
	Mustelidae	*Martes martes*	STIPB unnumbered specimen	C	Ar	1,300
		Mustela putorius	STIPB unnumbered specimen	C	Te	809
	Ursidae	*Ursus americanus*	MNHN-ZM-MO-1902-1415	E	Te	132,405
Cingulata	Dasypodidae	*Dasypus novemcinctus*	MNHN-ZM-MO-2001-1317	C	Te	3,949
Diprotodontia	Macropodidae	*Macropus giganteus*	MNHN-ZM-AC-A10098	C	Te	41,455
		Thylogale stigmatica	umzc:vertebrates:a12.44/1*	C	Te	4,306
	Potoroidae	*Aepyprymnus rufescens*	msu:mr:mr.4680*	C	Fo	2,820
	Vombatidae	*Vombatus ursinus*	MNHN-ZM-AC-A3289	C	Fo	25,750
Eulipotyphla	Erinaceidae	*Erinaceus europaeus*	STIPB unnumbered specimen	C	Te	778

	Solenodontidae	*Solenodon paradoxus*	MNHN-ZM-MO-1980-237	C	Fo	900
	Talpidae	*Euroscaptor micrura*	MNHN-ZM-MO-1959-1795	M	Fo	60
		Talpa europaea	MNHN-ZM-MO-1953-829	M	Fo	110
		Talpa europaea	STIPB unnumbered specimen	M	Fo	110
Monotremata	Ornithorhynchidae	*Ornithorhynchus anatinus*	MNHN-ZM-AC-1906-484	S	Aq	1,225
	Tachyglossidae	*Tachyglossus aculeatus*	MNHN-ZM-AC-1884-1125	S	Fo	3,170
Pholidota	Manidae	*Smutsia temminckii*	MNHN-ZM-AC-1897-134	C	Te	9,587
Primates	Cercopithecidae	*Chlorocebus aethiops*	MNHN-ZM-AC-1909-262	E	Ar	5,104
		Macaca radiata	MNHN-ZM-AC-1845-271	E	Ar	5,132
	Hominidae	*Pan paniscus*	amnh:mammals:m-202870*	E	Ar	35,120
	Lemuridae	*Lemur catta*	MNHN-ZM-AC-1910-101	C	Ar	2,555
Rodentia	Dipodidae	*Allactaga elater*	UF:mammal:30045*	C	Fo	59
		Dipodomys ordii	MNHN-ZM-MO-1958-294	C	Fo	50
		Zapus princeps	uwbm:mammal specimens:74482*	C	Te	28
		Zapus trinotatus	uwbm:mammal specimens:OG-7813*	C	Te	27
	Hystricidae	*Hystrix cristata*	MNHN-ZM-AC-1922-386	C	Fo	19,167
	Muridae	*Gerbillus campestris*	MNHN-ZM-MO-1990-10	C	Fo	28
		Meriones libycus	MNHN-ZM-MO-1981-619	C	Fo	91
	Pedetidae	*Pedetes capensis*	MNHN-ZM-AC-1883-1640	C	Fo	2,775
	Sciuridae	*Marmota marmota*	STIPB unnumbered specimen	C	Fo	3,500
Scandentia	Tupaiidae	*Tupaia belangeri*	STIPB unnumbered specimen	C	Ar	200
Tubulidentata	Orycteropodidae	*Orycteropus afer*	MNHN-ZM-AC-1919-19	C	Fo	56,175

141

142 is more abducted than in erect mammals (between 15 and 30 degrees relative to the parasagittal
143 plane; Jenkins 1971); and the humerus is also more horizontal, with the elbow oscillating from
144 about 20 degrees above the shoulder joint to 45 degrees below it. Both erect and crouched taxa
145 belong to the same morpho-functional continuum, with graviportal and cursorial taxa
146 representing the two extreme morphologies (Carrano 1999).

147 Besides this general pattern, some taxa have atypical humeral postures. The monotremes
148 *Tachyglossus* and *Ornithorhynchus* have more "sprawling" humeri, akin to what exists in extant

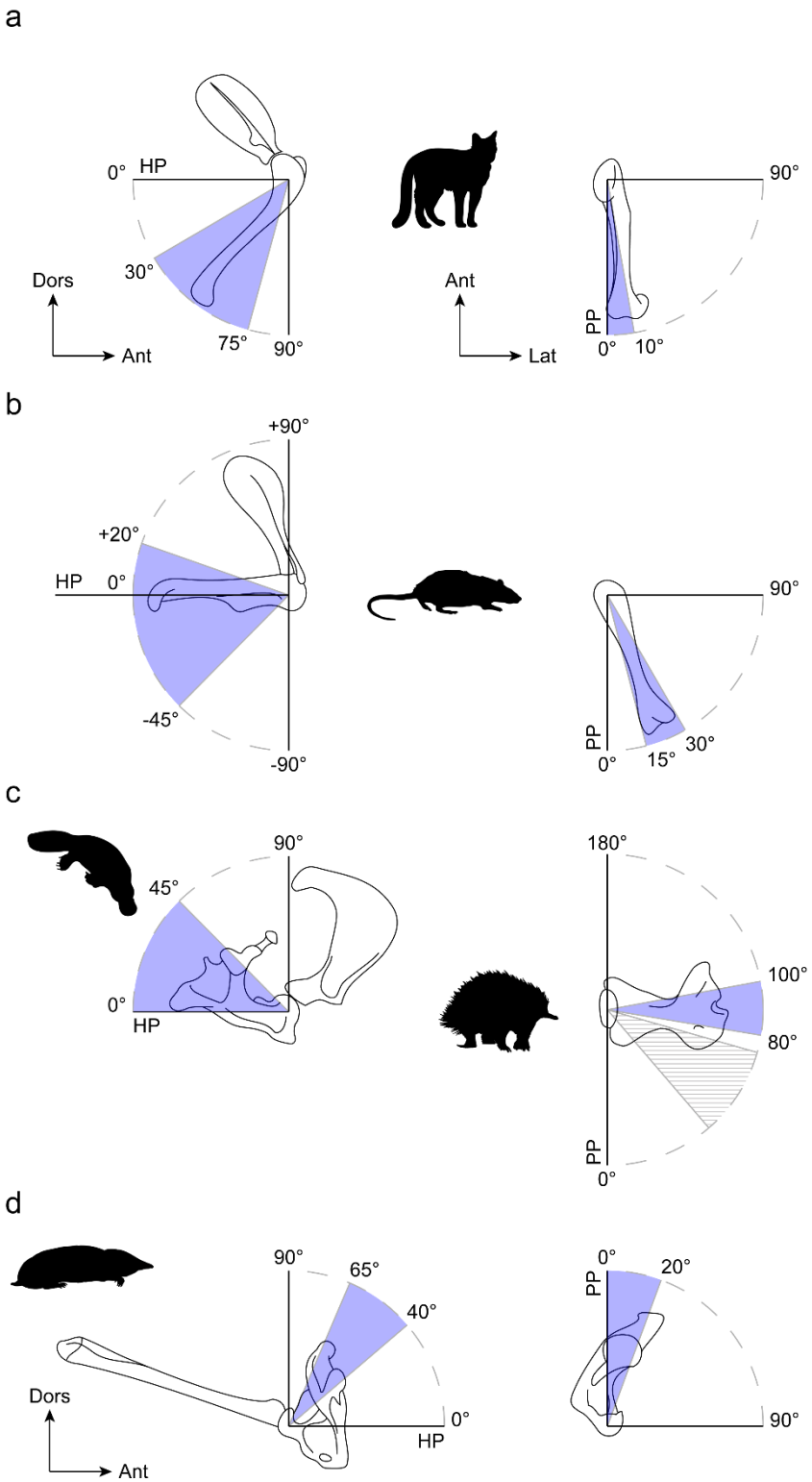

149 **Fig. 1** Humeral excursion at the shoulder joint in lateral (left) and dorsal (right) views in several
150 mammals with different postures (Jenkins 1971; Pridmore 1985; Lin et al. 2019). The scapula
151 and humerus are shown in lateral view, but the scapula is not shown in dorsal view for better
152 visibility of the humerus. a. erect humerus in *Felis domestica*; b. crouched humerus in *Rattus*
153 *norvegicus*;c. sprawling humerus in *Ornithorhynchus* (left and hatched area on right) and

Tachyglossus (right); d. modified humerus in *Scalopus aquaticus*. Abbreviations: HP, horizontal plane; PP, parasagittal plane. Silhouettes come from phylopic.org

ectothermic reptiles (Bakker 1971; but see Pridmore 1985; Gambaryan and Kuznetsov 2013). In *Tachyglossus*, the humerus is completely horizontal. The elbow oscillates laterally between 80 and 100 degrees from the parasagittal plane (Jenkins 1971; Pridmore 1985). In *Ornithorhynchus*, the humerus is abducted between 40 and 75 degrees from the parasagittal plane, with the elbow operating above the shoulder joint up to 45 degrees from the horizontal (Pridmore 1985). The forelimb of moles (Talpidae) is also highly modified in relation to their burrowing behaviour. The humerus is slightly abducted (less than 20 degrees from the parasagittal plane). The elbow oscillates cranially relative to the shoulder joint, rising 40 to 65 degrees from the horizontal plane (Lin et al. 2019).

DATA ACQUISITION

We measured various geometric and microanatomical parameters that have been previously associated in the literature with locomotion and posture, and more generally with lifestyle in amniotes (Canoville and Laurin 2009, 2010; Amson et al. 2014; Houssaye et al. 2016b; Houssaye and Botton-Divet 2018; Scheidt et al. 2019). This was done on cross-sections of mammalian humeral shafts obtained mainly from CT data retrieved from the literature and from morphosource.org. We scanned some of the specimens on the AST-RX platform of the Muséum national d'histoire naturelle and on the MRI platform of the Université de Montpellier. We extracted a cross-section from the CT data where the perimeter of the shaft was the smallest because this is an area where mechanical stresses generally are important (Beck et al. 1996; Tommasini et al. 2005; Campione and Evans 2012), resulting in more or less mid-diaphyseal cross-sections. We also incorporated into our data mid-diaphyseal traditional histological sections (unpublished data from Quemeneur et al. 2013). Mixing sections with slightly different reference planes in comparative studies is not considered a problem as long as the species of interest does not show excessive longitudinal microanatomical variation (Amson and Kolb 2016; Houssaye et al. 2018). The scans were processed in ImageJ (Abràmoff et al. 2004) and MorphoDig (Lebrun 2018). Each bone was oriented so that the section plane was as perpendicular as possible to the long axis of the diaphysis. Data for all left humeri were symmetrised so that the sample consisted of right side bones only. We binarised the cross-sections before taking our geometric and microanatomical measurements in ImageJ with the BoneJ plugin (Doube et al. 2010) and in R (R Core Team 2013) with the BoneProfileR package

(Girondot and Laurin 2003; Gônet et al. 2022). A sample of the mammalian cross-sections used in this study are presented in Fig. 2.

We measured six geometric parameters with BoneJ (Fig. 3): Pe_{min}, the minimum perimeter of the shaft; BCSA, the area occupied by the bone on the section; TCSA, the total area of the section; Ecc, the eccentricity of the section corresponding to the ratio of the area moments of inertia (I) around the major and minor axes (I_{max}/I_{min}); SR, the slenderness ratio (a high SR indicates a slender bone, while a low SR indicates a more robust bone; see Eq. 1); Z_{pol}, the polar section modulus reflecting the resistance of the shaft to torsion (the higher Z_{pol}, the more resistant the bone will be to torsion). Although Z_{pol} can be used with subcircular cross-sections, which is the case for most taxa, it is ideally used with circular cross-sections.

$$\text{Slenderness ratio} = \frac{\text{Bone length}}{\sqrt{\frac{I_{min}}{TCSA}}} \qquad (1)$$

We used BoneProfileR to measure seven microanatomical parameters (Fig. 3). We set BoneProfileR to determine the position of the centre of unmineralisation, i.e. the centre of the unmineralised spaces in the bone section, and segment the cross-section into 100 concentric circles. Bone compactness (measured by the number of bone pixels relative to the total number of pixels) was measured in each circle from the centre of the medulla to the edge of the cross-section. We extracted several parameters from the resulting compactness profiles: P, the distance of the medullo-cortical transition from the centre of the cross-section (a high P generally reflects low bone compactness); S, the inverse of the asymptote of the slope at point P (a high S corresponds to a gradual transition between the medulla and the cortex, as in the case of cancellous bone, while a low S reflects an abrupt transition). BoneProfileR also computes an observed global compactness value, C_{obs}. In addition, we performed a radial analysis to extract the radial component of the parameters P and S: the cross-section is segmented into 60 slices of 6 degrees and a compactness profile is drawn for each slice. The radial component of P (RP) and S (RS) is the average of the P and S of all slices. The standard deviation associated with RP and RS is RPSD and RSSD, respectively. When a species in our sample was represented by more than one individual, we calculated the mean value for each microanatomical parameter.

BUILDING REFERENCE PHYLOGENIES

We constructed a set of 100 reference trees of mammals to include phylogenetic uncertainty in our statistical analyses (Fig. 2). The trees were manipulated in R using the packages phytools

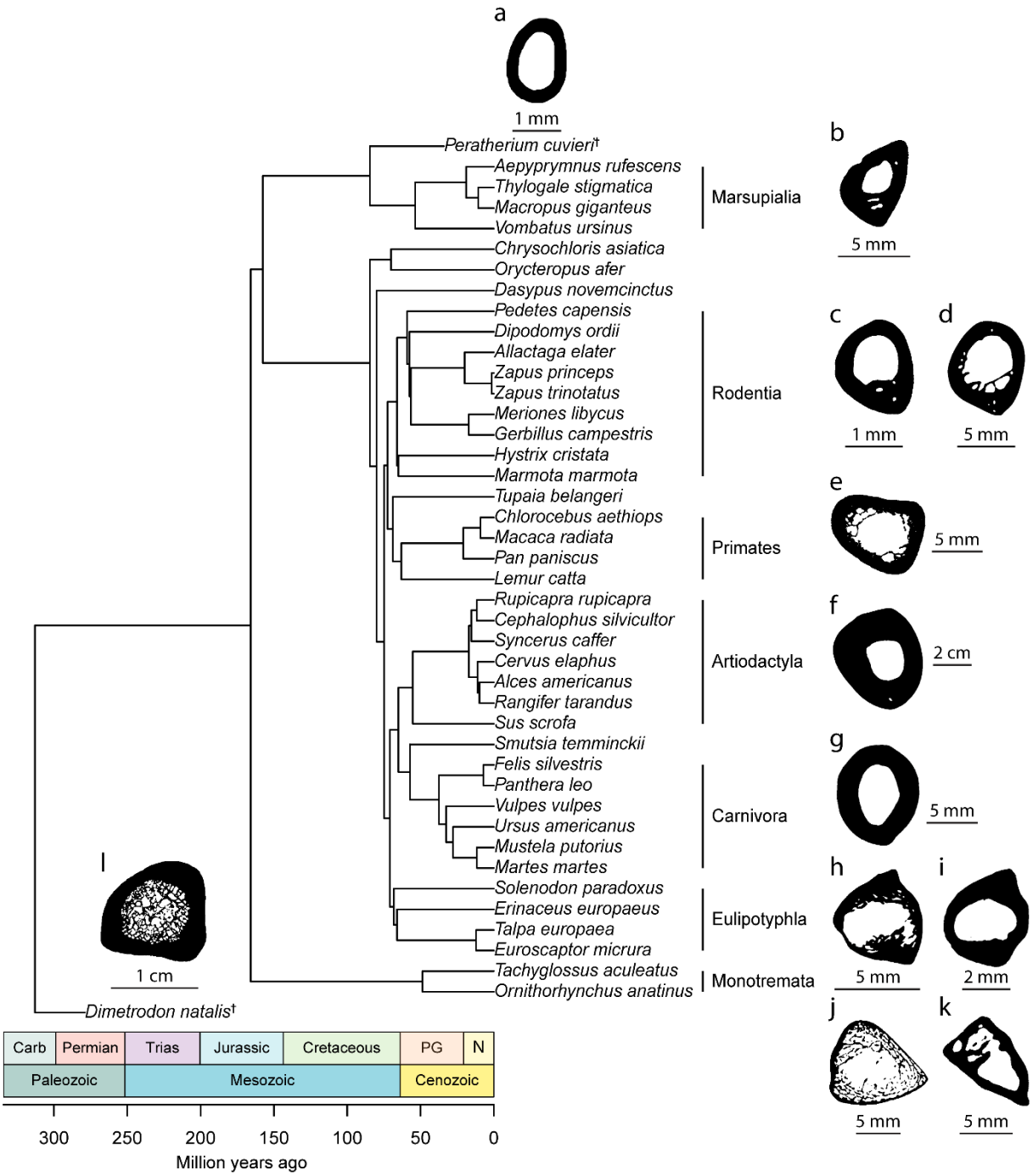

Fig. 2 Tree 1 of our set of 100 time-calibrated composite phylogenies displaying the evolutionary relationships among the extant and extinct species included in this study, with some of the humeral cross-sections analysed. a. *Peratherium cuvieri*† (Late Eocene) MNHN-F-GY679b (unknown); b. *Aepyprymnus rufescens* MorphoSource: msu:mr:mr.4680 (crouched); c. *Meriones libycus* MNHN-ZM-MO-1981-619 (crouched); d. *Marmota marmota* STIPB unnumbered specimen (crouched); e. *Macaca radiata* MNHN-ZM-AC-1845-271 (crouched); f. *Syncerus caffer* NHMUK ZD 1874.11.2.4 (erect); g. *Felis silvestris* UFGK unnumbered specimen (erect); h. *Talpa europaea* MNHN-ZM-MO-1953-829 (modified); i. *Euroscaptor micrura* MNHN-ZM-MO-1959-1795 (modified); j. *Tachyglossus aculeatus*

MNHN-ZM-AC-1884-1125 (sprawling); k. *Ornithorhynchus anatinus* MNHN-ZM-AC-1906-484 (sprawling); l. *Dimetrodon natalis*† (Early Permian) IPBSH-4 (unknown). The cross-sections are anatomically oriented (anterior to the top and lateral to the right) except for *Dimetrodon*. Trees were compiled in R using the work of Selva (2017), Upham et al. (2019), and Didier and Laurin (2020)

(Revell 2012) and TreePar (Stadler 2011). We extracted 100 trees with only the species of interest from a distribution of 10 000 Bayesian supertrees of mammals calibrated in time (node-dating, 5911 species) from the publication of Upham et al. (2019) and available on vertlife.org. The statistical analyses in this study required reference trees that included the taxa for which we wanted to infer posture. Therefore, *Dimetrodon natalis* (Sphenacodontidae) was branched at 313 Ma based on Didier and Laurin (2020). We followed Selva (2017) in considering *Peratherium cuvieri* an herpetotheriid and set the age of divergence between Herpetotheriidae and Marsupialia at approximately 85 Ma. The trees in Newick tree format are provided in Online Resource 2

BODY MASS ESTIMATES AND LIFESTYLE

Body mass affects posture and bone microanatomy. Indeed, among mammals, the largest taxa tend to have more erect/upright limbs and greater bone compactness (Biewener 1989b, 2005; Hutchinson 2021). We therefore collected body mass estimates from the literature for each taxon in our sample (Table 1; Online Resource 1). We relied entirely on the database of Myhrvold et al. (2015), which compiles median body mass for a large number of extant amniotes (we rounded values to the nearest gram).

Lifestyle is also known to be related to bone microanatomy, e.g., fossorial talpids have greater extension of the medullo-cortical transition compared to terrestrial talpids (Meier et al. 2013). Thus, we defined four lifestyle categories based on limb use (semi-aquatic, terrestrial, fossorial, and arboreal) to explore the potential relationship between lifestyle and posture (Table 1; Online Resource 1).

STATISTICAL TREATMENT IN A PHYLOGENETIC FRAMEWORK

Phylogenetic signal–We used the phylosig function from the R package phytools (Revell 2012) to estimate the phylogenetic signal in each geometric and microanatomical parameters. The phylosig function computes the K-statistic of Blomberg et al. (2003). A K-statistic greater than 1 indicates that closely related species in the tree show more similarity between them than what

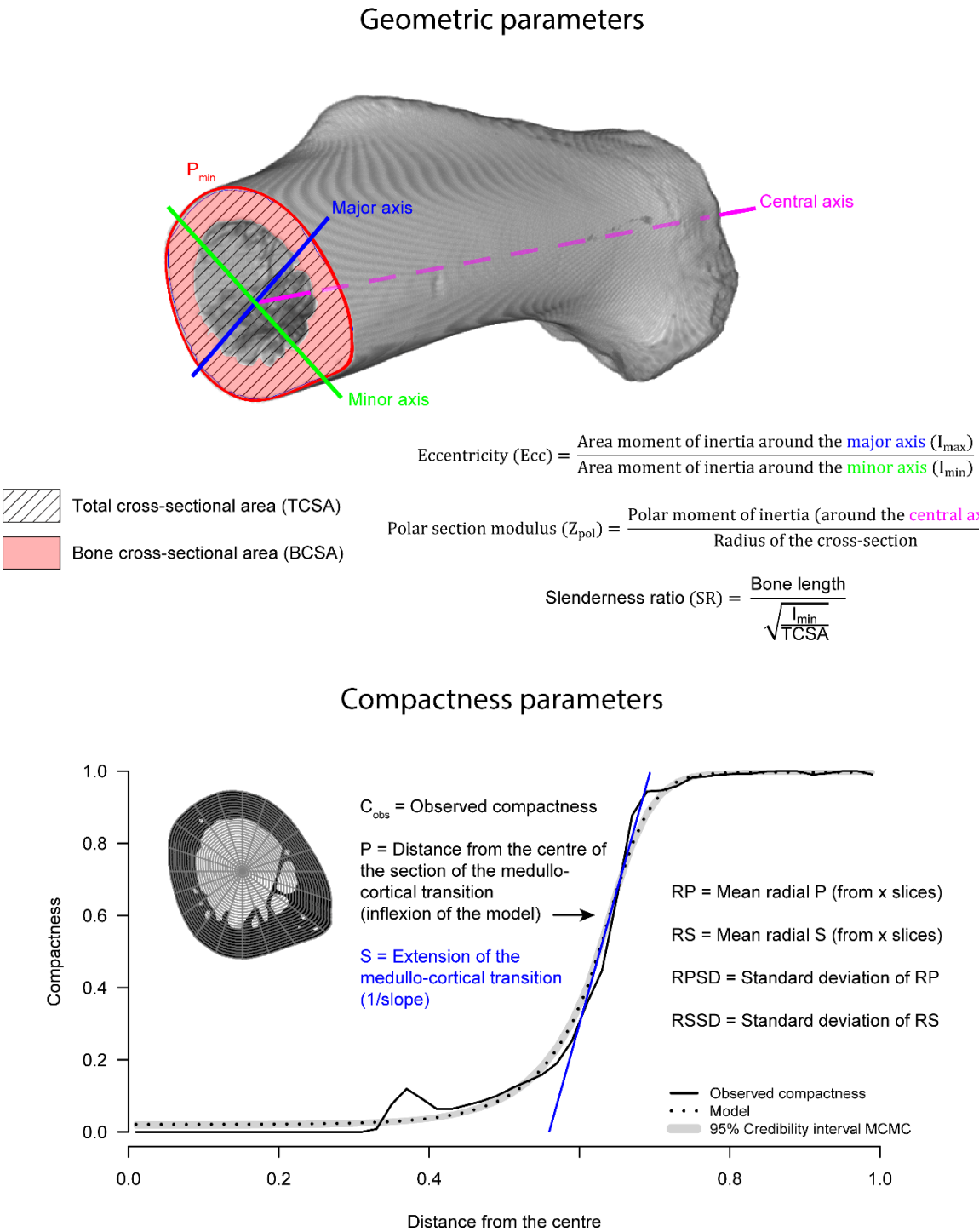

Fig. 3 All the geometric and compactness parameters measured in this study, illustrated here with a humerus of *Marmota marmota* (STIPB unnumbered specimen). The section on the compactness profile is divided into 30 concentric circles and 20 slices for better readability, but more were used in the analyses (100 and 60, respectively)

would be expected with a Brownian model of evolution, suggesting the existence of a substantial phylogenetic signal in the data. Conversely, a K-statistic lower than 1 implies that

closely related species are more different than expected highlighting evolutionary convergence or higher variance between clades rather than within them.

We used the delta-statistic (Borges et al. 2019), which was designed for categorical traits, to estimate the phylogenetic signal in posture. The delta-statistic depends on the uncertainty associated with the inference of ancestral states: low uncertainty implies low entropy (Shannon 1948) and a high delta-statistic. The higher the delta, the stronger the phylogenetic signal.

A *P*-value is obtained by randomisation, i.e. a redistribution of the measured traits among terminal branches. K and delta are computed 1000 and 100 times, respectively, with a random distribution, then the pool of values obtained is compared to the K and delta with the actual distribution. This was done for each tree in our phylogenetic tree sample.

Generalised least squares–We used the gls function from the R package nlme (Pinheiro et al. 2021) to model the relationship between each geometric and microanatomical parameter and postural groups while accounting for phylogeny, body mass and lifestyle. The gls function fits a linear model using least squares to optimise coefficients and allows a covariance structure to be set between observations. Here, the expected covariance of a given trait (or a relationship between traits) between two taxa corresponds to its evolution under a Brownian motion during the time from the root to their last common ancestor.

Phylogenetic flexible discriminant analysis–We used phylogenetic flexible discriminant analysis (PFDA) to explain posture in our sample of extant mammals and to predict humeral posture in *Dimetrodon* and *Peratherium* based on geometric and microanatomical measurements taken from humeral cross-sections while accounting for phylogeny. PFDA is a classification model based on a combination of linear regressions. It is derived from flexible discriminant analysis (FDA; Hastie et al. 1994) and corresponds to its phylogenetically informed version (Motani and Schmitz 2011). In practice, PFDA corresponds to a gls where categories are split in dummy variables and treated as continuous variables while phylogeny is incorporated as a phylogenetic covariance matrix whose terms are multiplied by lambda to make phylogenetic inertia variable through model optimisation (Pagel 1999). Lambda is assigned a value between 0 and 1 that minimises the model error, that is, the share of variance explained by phylogeny: 0 indicating that phylogeny does not explain the distribution of the trait on the tree; 1 indicating that phylogeny explains as much variance in the trait as is expected under a Brownian model of evolution.

Overfitting occurs when a model becomes overly complex by including too many parameters (Everitt and Skrondal 2010). An overfitted model will perform well in explaining initial data (training) but will perform poorly with new data or predictions (testing). The key to preventing overfitting lies in optimising the choice of parameters to include in the model in order to minimise test error. We chose the percentage of correct classification (PCC) obtained through leave-one-out cross-validation (CV; Stone 1974) as our selection criterion. The higher the PCC, the better the model performed under test conditions. Prior to performing CV procedures, we generated a dissimilarity matrix from the correlation coefficients of the geometric and microanatomical parameters before performing a hierarchical cluster analysis to identify and eliminate highly correlated variables (correlation coefficient > 0.95) in order to avoid subsequent complications related to the existence of singular variance-covariance matrices. Pe_{min}, BCSA, TCSA and Z_{pol} were all inter-correlated. We decided to keep only the parameter Pe_{min} which, in a paleobiological inference context, is the easiest to measure and least likely to be impacted by taphonomy. The parameters P and RP were also correlated. We kept the former and removed the latter from our data set. CV was performed with all possible combinations of the remaining parameters (Pe_{min}, Ecc, SR, C_{obs}, P, S, RS, RPSD and RSSD) and for each of the 100 phylogenetic trees for a total of more than 50,000 CV. In the end, only three parameters out of the original 13 were retained for our humerus inference model (Pe_{min}, SR and P). The R script and associated R environment allowing to replicate the postural inferences presented in the results of this study and allowing new inferences to be produced in other extinct synapsids from our dataset are available in Online Resources 3 and 4, respectively.

We then designed linear models in R to examine the association of the coordinates of the sampled taxa on the first and second axis of the PFDA model with body mass and lifestyle. When lifestyle was significant, we performed pairwise post-hoc tests with false discovery rate (FDR) correction using the emmeans_test function in the R package rstatix (Alboukadel 2021).

Results

PHYLOGENETIC SIGNAL IN THE DATA

All geometric parameters except for cross-sectional eccentricity (Ecc) were significantly associated with phylogeny (Table 2). For Pe_{min}, BCSA, TCSA and Z_{pol}, the K-statistic was below 1, indicating that intra-clade variation is greater than inter-clade variation and suggesting patterns of evolutionary convergence. However, K was close to 1 for the slenderness ratio (SR), implying that the distribution of this trait on the phylogeny is consistent with what would be

expected under a Brownian model of evolution and therefore reflects a phylogenetic signal. S and RPSD were the only microanatomical parameters to be significantly associated with phylogeny (Table 2). K was lower than 1 in each case, highlighting convergences. Posture also contained a substantial phylogenetic signal (*P*-value < 0.01), with the delta-statistic ranging from 3.194 to 21.471 (mean = 11.982; see Table 2).

Table 2 Phylogenetic signal in the data. Values reported in the table are means obtain from 100 phylogenetic trees. The *P*-values for K (Blomberg et al. 2003) and delta (Borges et al. 2019) are obtained from 1000 and 100 randomisations, respectively. Minimum and maximum values obtained from our distribution of 100 phylogenetic trees are given in parentheses. All geometric and microanatomical parameters, except ratios, were log-transformed in R

Parameter	K-statistic	Delta-statistic	*P*-value
Pe_{min}	0.58 (0.506–0.706)		0.001** (0.001–0.003)
BCSA	0.616 (0.536–0.745)		0.001** (0.001–0.003)
TCSA	0.593 (0.517–0.72)		0.001** (0.001–0.002)
Ecc	0.185 (0.1-0.251)		0.403 (0.194–0.63)
Z_{pol}	0.611 (0.531–0.742)		0.001** (0.001–0.002)
SR	0.915 (0.796–1.069)		0.001** (0.001–0.001)
P	0.237 (0.15–0.298)		0.151 (0.051–0.334)
S	0.392 (0.339–0.472)		0.007** (0.002–0.017)
C_{obs}	0.169 (0.078–0.254)		0.52 (0.177–0.781)
RP	0.225 (0.144–0.279)		0.186 (0.092–0.359)
RS	0.272 (0.237–0.332)		0.059 (0.03–0.105)
RPSD	0.697 (0.586–0.813)		0.001** (0.001–0.003)
RSSD	0.234 (0.2-0.274)		0.159 (0.081–0.278)
Posture		11.982 (3.194–21.471)	< 0.001*** (< 0.001–0.01)

GEOMETRIC AND MICROANATOMICAL COMPARISON OF POSTURAL GROUPS

The microanatomical parameter S and the geometric parameters Pe_{min}, BCSA, TCSA, Zpol and SR are all significantly associated with posture (Table 3). They were also always significantly related to body mass and never to lifestyle except for SR and S, which are significantly associated with both body mass and lifestyle. RPSD was significantly associated only with

Table 3 Effect of posture, body mass and functional ecology/lifestyle on the humeral geometric and microanatomical parameters. Values reported are means obtained from 100 phylogenetic trees. Minimum and maximum values obtained from our distribution of 100 phylogenetic trees are given in parentheses. Body mass and all geometric and microanatomical parameters, except ratios, were log-transformed in R. Abbreviations: BM, body mass; LS, lifestyle; POS, posture

GLS model formula	Independent variables	Chi-square values	*P*-values
Pe_{min} ~ BM + LS + POS	POS	14.653 (10.196–18.37)	0.003** (< 0.001–0.017)
	BM	536.358 (366.969-653.646)	< 0.001***
	LS	3.311 (2.21–4.439)	0.35 (0.218–0.53)
BCSA ~ BM + LS + POS	POS	13.884 (12.008–15.852)	0.003** (0.001–0.007)
	BM	551.749 (509.506-597.076)	< 0.001***
	LS	4.869 (4.208–5.937)	0.184 (0.115–0.24)
TCSA ~ BM + LS + POS	POS	18.178 (13.67-22.052)	< 0.001*** (< 0.001–0.003)
	BM	645.451 (478.171-755.691)	< 0.001***
	LS	4.688 (3.44–6.266)	0.2 (0.099–0.329)
Ecc ~ BM + LS + POS	POS	0.55 (0.274–0.987)	0.907 (0.804–0.965)
	BM	0.02 (< 0.001–0.161)	0.912 (0.689–0.999)
	LS	3.645 (2.009–5.04)	0.311 (0.169–0.571)
Z_{pol} ~ BM + LS + POS	POS	20.982 (18.529–23.534)	< 0.001***
	BM	794.205 (735.737-861.524)	< 0.001***
	LS	7.175 (5.93–8.665)	0.069 (0.034–0.115)
SR ~ BM + LS + POS	POS	15.664 (13.844–17.459)	0.001** (0.001–0.003)
	BM	13.869 (11.131–16.525)	< 0.001*** (< 0.001–0.001)
	LS	8.718 (7.529–10.025)	0.034* (0.018–0.057)
P ~ BM + LS + POS	POS	1.071 (0.614–1.524)	0.784 (0.677–0.893)
	BM	0.088 (0.003–0.248)	0.778 (0.619–0.956)
	LS	1.318 (0.848–1.788)	0.725 (0.617–0.838)
S ~ BM + LS + POS	POS	12.697 (11.016–14.076)	0.006** (0.003–0.012)
	BM	7.031 (6.033–8.012)	0.008** (0.005–0.014)
	LS	11.017 (9.13-13.989)	0.013* (0.003–0.028)
C_{obs} ~ BM + LS + POS	POS	1.288 (0.51–2.173)	0.733 (0.537–0.917)

	BM	0.063 (0.002–0.183)	0.812 (0.668–0.961)
	LS	2.529 (1.128–4.161)	0.478 (0.245–0.77)
RP ~ BM + LS + POS	POS	1.404 (0.826–1.963)	0.705 (0.58–0.843)
	BM	0.025 (< 0.001–0.134)	0.895 (0.714–0.999)
	LS	2.234 (1.449–2.94)	0.527 (0.401–0.694)
RS ~ BM + LS + POS	POS	4.919 (4.157–6.171)	0.18 (0.104–0.245)
	BM	9.705 (8.243–11.851)	0.002** (0.001–0.004)
	LS	6.89 (5.721–8.036)	0.077 (0.045–0.126)
RPSD ~ BM + LS + POS	POS	5.334 (4.365–6.047)	0.151 (0.109–0.225)
	BM	1.048 (0.373–2.005)	0.317 (0.157–0.541)
	LS	9.671 (8.443–11.623)	0.022* (0.009–0.038)
RSSD ~ BM + LS + POS	POS	2.482 (2.011–3.219)	0.48 (0.359–0.57)
	BM	5.234 (4.379–6.227)	0.023* (0.013–0.036)
	LS	3.955 (3.268–4.565)	0.268 (0.207–0.352)

lifestyle, RS and RSSD only with body mass.

PHYLOGENETIC DISCRIMINATION OF POSTURAL GROUPS

The PFDA model was very successful in discriminating between postural groups (Fig. 4). Indeed, the mean training PCC reached 88% (88-90%). Most of the time, crouched taxa were correctly classified at 83% (19 out of 23 taxa). The rest of the time (5% of the phylogenetic trees), they reached 87% (20 out of 23 taxa). With all tree hypotheses, the erect taxa were correctly classified at 93% (13 out of 14 taxa) while the two monotremes (sprawling) and the two talpids (modified) both achieved 100% of correct classifications. *Dimetrodon* and *Peratherium* were always inferred as sprawling and crouched, respectively. Lambda ranged from 0.04 to 0.17 (mean = 0.099), indicating a present but low influence of the phylogeny.

Body mass was significantly associated with the taxon coordinates on the first and second PFDA axes (Table 4). Lifestyle was significantly associated with the taxon coordinates on the first PFDA axis but not on the second, although the *P*-values were close to the significance level. The results of the post-hoc tests with the first PFDA axis revealed that arboreal taxa were significantly different from semi-aquatic, terrestrial and fossorial taxa, and that fossorial taxa were significantly different from terrestrial taxa (Table 5).

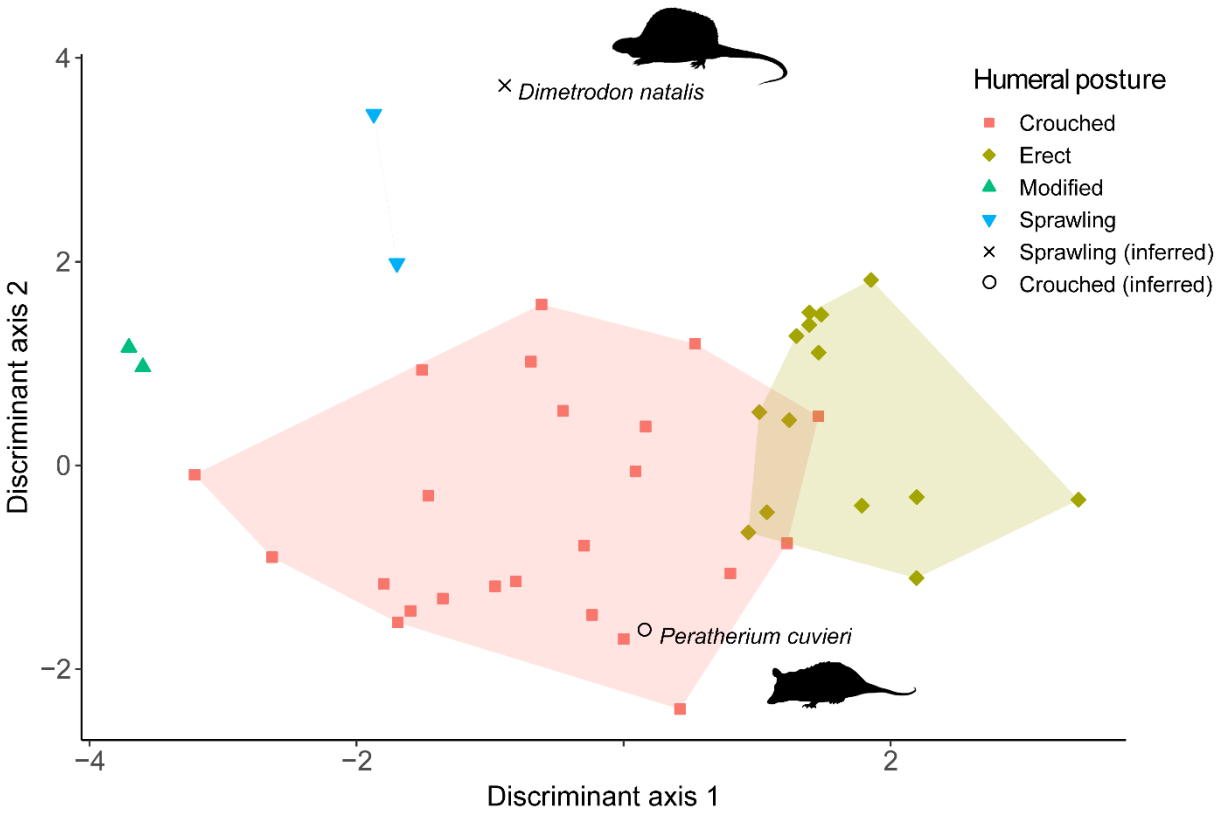

Fig. 4 Phylogenetic discriminant space generated from PFDA (Motani and Schmitz 2011) on postural groups. Based on posterior probabilities, *Dimetrodon* and *Peratherium* are inferred as "sprawling" and "crouched", respectively. Silhouettes come from phylopic.org

Discussion

Cross-sectional characterisation of postural groups

Pe_{min}, BCSA, TCSA were all significantly associated with posture (Table 3). This is not surprising since Pe_{min} is related to body mass (Campione and Evans 2012), and it is well known that body mass and limb posture in mammals are related (Biewener 1989b, 2005; Houssaye et al. 2016b). Indeed, large mammals tend to have more erect (columnar) limbs that help reduce tissue stress (Gregory 1912; Biewener 1989a, Gatesy and Biewener 1991; Hutchinson 2021). This is because bone resists compression better than tension or torsion (Currey 2013). Logically, Pe_{min} increases with increasing bone size and so do both BCSA and TCSA. The significant association between Z_{pol} and posture is interesting, as it probably reveals a difference in torsional strength in the humerus between postures. Indeed, previous studies, including in-vivo measurements, have shown that crouched taxa, just like non-avian reptiles with a sprawling posture, exhibit increased torsional stress compared to erect taxa, which are primarily loaded in bending (Biewener 1990; Blob and Biewener 1999, 2001; Butcher et al. 2008, 2011). SR and S are the only parameters to be significantly associated with both posture and lifestyle.

Table 4 Effect of body mass and lifestyle on the taxon coordinates on the first and second axes of the PFDA model. Values reported are means obtained from 100 phylogenetic trees. Minimum and maximum values obtained from our distribution of 100 phylogenetic trees are indicated in parentheses. Abbreviations: BM, body mass; LS, lifestyle

Linear model formula	Independent variable	F-value	*P*-value
Coordinates of the taxa on the first PFDA axis ~ BM + LS	BM	53.88 (46.071–57.117)	< 0.001***
	LS	11.807 (11.244–12.138)	< 0.001***
Coordinates of the taxa on the second PFDA axis ~ BM + LS	BM	14.499 (13.927–15.613)	< 0.001*** (< 0.001–0.001)
	LS	2.7 (2.526–2.767)	0.06 (0.056–0.073)

Table 5 Differences in taxon coordinates on the first PFDA axis between lifestyle categories as shown by pairwise comparison. Values reported are means obtained from 100 phylogenetic trees. Minimum and maximum values obtained from our distribution of 100 phylogenetic trees are indicated in parentheses. Abbreviations: Aq, semi-aquatic; Ar, arboreal; Fo, fossorial; Te, terrestrial

Pairwise comparison	Adjusted *P*-value
Aq vs. Ar	0.006** (0.005–0.007)
Aq vs. Fo	0.547 (0.533–0.563)
Aq vs. Te	0.161 (0.145–0.171)
Ar vs. Fo	< 0.001***
Ar vs. Te	0.001** (< 0.001–0.001)
Fo vs. Te	0.028* (0.023–0.036)

Monotremes and talpids have some of the most robust humeri. These taxa are also the most fossorial species in our sample. This is because burrowing habits generally go hand in hand with robust, stocky forelimbs for digging in hard substrates (Shimer 1903). Similarly, the primates in our sample have the slenderest humeri. They are also the species with the most arboreal habits. Indeed, arboreal species generally have slender, elongated forelimbs that allow them to move more efficiently in trees by increasing reach and reducing energy expenditure during vertical climbing, as longer arms allow them to lean back more, thereby increasing friction between the foot and the substrate (Preuschoft et al. 1996; Isler 2005). The talpids show

the highest S values in the sample. Two reasons can explain these high S values: (1) The presence of cancellous bone considerably extending the transition between the medulla and the cortex. The corresponding compactness profile is flattened, resulting in a low slope of the asymptote at point P and thus a high S value (S = 1/slope). (2) Heterogeneity of cortical thickness. Variations in cortical thickness depending on the position within the cross-section mimic an extensive transition between the medulla and the cortex on the overall compactness profile. Talpids clearly show a thickening of the cortex antero-posteriorly (Fig. 2). An increase in mechanical stress in these regions, due to the attachment of strong muscles involved in the adduction/abduction cycle of the humerus (Rose et al. 2013), could explain these variations in cortical thickness.

PHYLOGENETIC DISCRIMINANT MODEL AND PALAEOBIOLOGICAL INFERENCES

Lambda was always greater than 0, indicative of a phylogenetic involvement in the PFDA, which attempts to maximise the relationships between humeral posture and the microanatomical parameters. This result is far from being surprising. Indeed, we saw that humeral posture was significantly associated with phylogeny (Table 2). Nevertheless, this confirmsour choice to use a classification method accounting for species relatedness. With a mean correct classification rate exceeding 85%, the PFDA model was very successful in discriminating the postural groups. Even monotremes and talpids, represented by only four individual taxa (*Ornithorhynchus* and *Tachyglossus*, and *Euroscaptor* and *Talpa*, respectively), are always correctly classified.

The Late Eocene herpetotheriid *Peratherium cuvieri* was inferred to be "crouched" with all trees in our phylogenetic tree sample. Studies on herpetotheriid locomotion are very sparse. Kurz (2005) designated *Amphiperatherium* and another undetermined herpetotheriid as "cursorial" based on lumbar vertebral morphology and tail length. Horovitz et al. (2008) described *Herpetotherium* as "agile" based on femoral morphology. The literature is more abundant regarding their extant close relatives, the Didelphidae. The didelphids are commonly used as models to study the evolution of therian locomotion (Jenkins 1971; Jenkins and Weijs 1979; Argot 2001; Butcher et al. 2011). Didelphids, like most small mammals, have a crouched posture (Jenkins 1971). Thus, a crouched posture in *Peratherium cuvieri* is deemed very plausible.

The posture of permo-carboniferous synapsids (the earliest stem mammals) has been extensively studied, in comparison to that of herpetotheriids. Indeed, it is widely accepted,

based on anatomical, biomechanical, and ichnological evidence, that the earliest stem mammals had sprawling limbs (Jenkins 1973; Hunt and Lucas 1998; Blob 2001; Benton 2015; Hopson 2015; Wright 2018; Cavanaugh 2021). Therefore, it is not surprising that *Dimetrodon natalis* was inferred to be a sprawler by the PFDA model, although the posturalhas not yet been clearly established. Sometimes described as "lizard-like" (Bakker 1971; Desmond 1975), the sprawling posture of monotremes may in fact be close to the ancestral condition of synapsids, yet distinct from the sprawling posture of squamates and urodeles (Gambaryan and Kuznetsov 2013; Regnault et al. 2020), or it may be derived from early mammals with parasagittal limbs (Pridmore 1985). Similarly in reptiles, Crocodylia, with their "semi-erect" limbs, were commonly considered "primitive" posturally (Bakker 1971; Charig 1972), when in fact they are descended from more erect forms (Parrish 1987; Gatesy 1991; Reilly and Elias 1998).

Body mass seems to have a confounding effect on our PFDA model (Table 4). This is not surprising since the parameter Pe_{min} was used in the model. We have already mentioned that body mass and posture in mammals are strongly intertwined. But we do not see this as a problem, on the contrary. Indeed, our goal is to build a model that can effectively discriminate between humeral postures in mammals based on easily measurable parameters, including in fossils, so that inferences can be produced for extinct taxa. If body mass is a powerful parameter to achieve this goal, we should use it by including, or rather not excluding, parameters associated with it, such as the perimeter of the cross-section. However, body mass, although useful, is not sufficient to distinguish between postures. Indeed, some species have equivalent body mass but different posture; e.g. *Marmota* (crouched) and *Tachyglossus* (sprawling). It should also be mentioned here that some ungulates with erect limbs weigh less than 10 kg, e.g. dik-diks (genus *Madoqua*). The case of small ungulates, although beyond the scope of this study, is worthy of further investigation. Therefore, we believe that femoral geometric and microanatomical parameters contain a functional signal that a multivariate quantitative approach such as PFDA can effectively exploit. Lifestyle was significantly associated with the first axis of the model and was close to the significance level for the second axis. This is most likely due to the presence of SR in the model. Indeed, we saw that the slenderness ratio was significantly associated with both body mass, posture, and lifestyle.

Post-hoc tests revealed that virtually all lifestyle categories were significantly different on the first axis with the exception of semi-aquatic taxa (Table 5). However, the only semi-aquatic taxon in our analysis was *Ornithorhynchus*. Therefore, this is most likely due to the small sample size, which results in a lack of statistical power. However, semi-aquatic taxa, such

as otters, deserve a separate study, as they tend to show pachyostosis and/or osteosclerosis (an increase in periosteal bone deposits and widespread spongiosa, respectively), which affect buoyancy (Houssaye et al. 2016a).

At first glance, it is surprising that S was not retained in the PFDA model since it seems to be significantly associated with posture unlike P (Table 3). However, the result of the cross-validation with the parameters Pe_{min}, SR and S gives only 73% of correct classification (15% less compared to the original model). Ultimately, joint use of Pe_{min}, SR and P seems to be the best parameter configuration to discriminate mammalian posture with our sample.

Conclusion

Using generalised least squares, we showed that all parameters that were significantly associated with posture, i.e. minimum humeral shaft perimeter (Pe_{min}), bone cross-sectional area (BCSA), total cross-sectional area (TCSA), polar section modulus (Z_{pol}), slenderness ratio (SR) and the reciprocal of the slope of the asymptote at point P on the compactness profile (S), were also significantly associated with body mass. This was expected as body mass is known to have an impact on posture in mammals, with smaller species having a crouched posture and larger species having more erect limbs to minimise body weight-induced stresses. The association between Z_{pol} and posture was also expected since Z_{pol} corresponds to the resistance of the shaft to torsion, and previous studies have shown that in mammals (and other taxa) crouched limbs are subject to higher torsional stresses than erect limbs, which are primarily loaded in flexion. We showed that SR and S were also related to lifestyle, with burrowing taxa having more robust humeri and arboreal taxa having slender humeri, and moles exhibiting heterogeneity in cortical thickness most likely related to the attachment of strong muscles on the anterior and posterior surfaces of the humerus involved in the limb adduction/abduction cycle.

A number of parameters were significantly associated with phylogeny (Pe_{min}, BSCA, TCSA, Z_{pol}, S and RPSD), as well as posture itself. The lambda values from the PFDA model indicated an influence of the phylogeny in the data, justifying the use of a phylogenetically informed classification method. Elimination of overly correlated parameters followed by cross-validation procedures ultimately yielded a PFDA model with three variables (Pe_{min}, SR and P) that successfully discriminated postural groups (88% average correct classification into four categories based on 100 mammalian phylogenetic trees). Despite the small sample size, the model was able to correctly classify moles (modified humeral posture) and monotremes

(sprawling humeral posture). Application of the model to extinct taxa yielded plausible results. *Peratherium cuvieri* and *Dimetrodon natalis* are inferred to have had a crouched and sprawling humeral posture, respectively. The PFDA model appeared to be significantly influenced by body mass and lifestyle, but nevertheless allows quantitative postural discrimination that size or lifestyle parameters alone would not achieve, while producing plausible inferences in extinct taxa.

Our study highlights the complex interplay between body mass, lifestyle, posture and the geometry and microanatomy of the humerus in mammals. Our model can be used by palaeontologists to infer the humeral posture of other extinct species based on humeral cross-sections alone. Extending our method to other appendicular skeletal elements could refine the inferences produced for extinct taxa, particularly those relevant to the context of shifts in limb posture (more sprawling to more erect/parasagittal limbs) in early mammals, which tend to exhibit a mosaic of characters.

Supplementary information–The online version contains supplementary material available at https://doi.org/10.1007/s10914-023-09652-w.

Acknowledgements–We warmly thank Alexandra Houssaye, Charlène Selva, Sandrine Ladevèze and Guillaume Billet for sharing with us the CT data of some of the studied specimens. We thank Joséphine Lesur, Géraldine Veron, Jacques Cuisin and Violaine Nicolas-Colin for granting us access to the MNHN collections. We are grateful to Renaud Lebrun and the MRI platform of the Université de Montpellier and to Marta Bellato and the AST-RX platform of the MNHN for their help in collecting CT data. We are indebted to Margot Michaud and Laura Bento Da Costa for their valuable advice and to Mathilde Aladini for her kind review of the manuscript. We are grateful to our two anonymous reviewers, whose comments helped to improve the quality of this study. We thank the Virtual Data initiative, run by the LabEx P2IO and supported by the Université Paris-Saclay, for providing computing resources on its cloud infrastructure.

Author contributions–JG collected the data, designed the study, performed the analyses, interpreted the results, wrote the manuscript. JB designed the analyses. MG designed the analyses. JRH interpreted the results. ML collected the data, designed the study, interpreted the results. All authors reviewed and approved the final manuscript.

Funding–This work was supported by the doctoral programme Interfaces pour le vivant (IPV), with the cooperation of Sorbonne Université, and by the ATM MNHN 2014 "formes possibles, formes réalisées".

Data availability–The data that support the findings of this study are included in this published article and its online resources.

Conflict of interest–The authors declare that they have no conflicts of interest.

References

Abbott CP (2019) The *Dimetrodon* dilemma: reassessing posture in sphenacodontians and related non-mammalian synapsids. Undergraduate honors dissertation, College of William and Mary

Abràmoff MD, Magalhães PJ, Ram SJ (2004) Image processing with ImageJ. Biophotonics Int 11:36–42

Alboukadel K (2021) rstatix: pipe-friendly framework for basic statistical tests. R package version 0.7.0

Amson E, Kolb C (2016) Scaling effect on the mid-diaphysis properties of long bones—the case of the Cervidae (deer). Sci Nat 103:1–10. https://doi.org/10.1007/s00114-016-1379-7

Amson E, de Muizon C, Laurin M, Argot C, de Buffrénil V (2014) Gradual adaptation of bone structure to aquatic lifestyle in extinct sloths from Peru. Proc R Soc Lond B Biol Sci 281:20140192. https://doi.org/10.1098/rspb.2014.0192

Argot C (2001) Functional-adaptive anatomy of the forelimb in the Didelphidae, and the paleobiology of the Paleocene marsupials *Mayulestes ferox* and *Pucadelphys andinus*. J Morphol 247:51–79. https://doi.org/10.1002/1097-4687(200101)247:1<51::AID-JMOR1003>3.0.CO;2-%23

Bakker RT (1971) Dinosaur physiology and the origin of mammals. Evolution 25:636–658. https://doi.org/10.1111/j.1558-5646.1971.tb01922.x

Beck TJ, Ruff CB, Mourtada FA, Shaffer RA, Maxwell-Williams K, Kao GL, Sartoris DJ, Brodine S (1996) Dual-energy X-ray absorptiometry derived structural geometry for

557 stress fracture prediction in male U.S. marine corps recruits. J Bone Miner Res 11:645–
558 653. https://doi.org/10.1002/jbmr.5650110512

559 Benton MJ (2015) Vertebrate Palaeontology. Wiley, Hoboken

560 Biewener AA (1989a) Mammalian terrestrial locomotion and size. Bioscience 39:776–783.
561 https://doi.org/10.2307/1311183

562 Biewener AA (1989b) Scaling body support in mammals: limb posture and muscle mechanics.
563 Science 245:45–48. https://doi.org/10.1126/science.2740914

564 Biewener AA (1990) Biomechanics of mammalian terrestrial locomotion. Science 250:1097–
565 1103. https://doi.org/10.1126/science.2251499

566 Biewener AA (2005) Biomechanical consequences of scaling. J Exp Biol 208:1665–1676.
567 https://doi.org/10.1242/jeb.01520

568 Bishop PJ, Hocknull SA, Clemente CJ, Hutchinson JR, Barrett RS, Lloyd DG (2018a)
569 Cancellous bone and theropod dinosaur locomotion. Part II—a new approach to
570 inferring posture and locomotor biomechanics in extinct tetrapod vertebrates. PeerJ
571 6:e5779. https://doi.org/10.7717/peerj.5779

572 Bishop PJ, Hocknull SA, Clemente CJ, Hutchinson JR, Farke AA, Barrett RS, Lloyd DG
573 (2018b) Cancellous bone and theropod dinosaur locomotion. Part III—inferring posture
574 and locomotor biomechanics in extinct theropods, and its evolution on the line to birds.
575 PeerJ 6:e5777. https://doi.org/10.7717/peerj.5777

576 Bishop PJ, Hocknull SA, Clemente CJ, Hutchinson JR, Farke AA, Beck BR, Barrett RS, Lloyd
577 DG (2018c) Cancellous bone and theropod dinosaur locomotion. Part I—an
578 examination of cancellous bone architecture in the hindlimb bones of theropods. PeerJ
579 6:e5778. https://doi.org/10.7717/peerj.5778

580 Blob RW (2000) Interspecific scaling of the hindlimb skeleton in lizards, crocodilians, felids
581 and canids: does limb bone shape correlate with limb posture? J Zool 250:507–531.
582 https://doi.org/10.1111/j.1469-7998.2000.tb00793.x

583 Blob RW (2001) Evolution of hindlimb posture in nonmammalian therapsids: biomechanical
584 tests of paleontological hypotheses. Paleobiology 27:14–38.
585 https://doi.org/10.1666/0094-8373(2001)0272.0.CO;2

586 Blob RW, Biewener AA (1999) In vivo locomotor strain in the hindlimb bones of *Alligator*
587 *mississippiensis* and *Iguana iguana*: implications for the evolution of limb bone safety
588 factor and non-sprawling limb posture. J Exp Biol 202:1023–1046.
589 https://doi.org/10.1242/jeb.202.9.1023

590 Blob RW, Biewener AA (2001) Mechanics of limb bone loading during terrestrial locomotion
591 in the green iguana (*Iguana iguana*) and American alligator (*Alligator mississippiensis*).
592 J Exp Biol 204:1099–1122. https://doi.org/10.1242/jeb.204.6.1099

593 Blomberg SP, Garland T, Ives AR (2003) Testing for phylogenetic signal in comparative data:
594 behavioral traits are more labile. Evolution 57:717–745. https://doi.org/10.1111/j.0014-
595 3820.2003.tb00285.x

596 Borges R, Machado JP, Gomes C, Rocha AP, Antunes A (2019) Measuring phylogenetic signal
597 between categorical traits and phylogenies. Bioinformatics 35:1862–1869.
598 https://doi.org/10.1093/bioinformatics/bty800

599 Brocklehurst N, Kammerer CF, Fröbisch J (2013) The early evolution of synapsids, and the
600 influence of sampling on their fossil record. Paleobiology 39:470–490.
601 https://doi.org/10.1666/12049

602 Brocklehurst RJ, Fahn-Lai P, Regnault S, Pierce SE (2022) Musculoskeletal modeling of
603 sprawling and parasagittal forelimbs provides insight into synapsid postural transition.
604 iScience 25:103578. https://doi.org/10.1016/j.isci.2021.103578

605 Butcher MT, Espinoza NR, Cirilo SR, Blob RW (2008) In vivo strains in the femur of river
606 cooter turtles (*Pseudemys concinna*) during terrestrial locomotion: tests of force-
607 platform models of loading mechanics. J Exp Biol 211:2397–2407.
608 https://doi.org/10.1242/jeb.018986

609 Butcher MT, White BJ, Hudzik NB, Gosnell WC, Parrish JH, Blob RW (2011) In vivo strains
610 in the femur of the Virginia opossum (*Didelphis virginiana*) during terrestrial
611 locomotion: testing hypotheses of evolutionary shifts in mammalian bone loading and
612 design. J Exp Biol 214:2631–2640. https://doi.org/10.1242/jeb.049544

613 Campione NE, Evans DC (2012) A universal scaling relationship between body mass and
614 proximal limb bone dimensions in quadrupedal terrestrial tetrapods. BMC Biol 10:1–
615 22. https://doi.org/10.1186/1741-7007-10-60

Canoville A, Laurin M (2009) Microanatomical diversity of the humerus and lifestyle in lissamphibians. Acta Zool 90:110–122. https://doi.org/10.1111/j.1463-6395.2008.00328.x

Canoville A, Laurin M (2010) Evolution of humeral microanatomy and lifestyle in amniotes, and some comments on palaeobiological inferences. Biol J Linn Soc Lond 100:384–406. https://doi.org/10.1111/j.1095-8312.2010.01431.x

Canoville A, de Buffrénil V, Laurin M (2021) Bone microanatomy and lifestyle in tetrapods. In: de Buffrénil V, de Ricqlès AJ, Zylberberg L, Padian K, Laurin M, Quilhac A (eds) Vertebrate Skeletal Histology and Paleohistology. CRC Press, Boca Raton, pp 724–743

Carrano MT (1999) What, if anything, is a cursor? Categories versus continua for determining locomotor habit in mammals and dinosaurs. J Zool 247:29–42. https://doi.org/10.1111/j.1469-7998.1999.tb00190.x

Cavanaugh T (2021) Reconstructing body size and center of mass in synapsids. Dissertation, Harvard University

Charig AJ (1972) The evolution of the archosaur pelvis and hindlimb: an explanation in functional terms. In: Joysey KA, Kemp TS (eds) Studies in Vertebrate Evolution. Oliver and Boyd, Edinburgh, pp 121–155

Cooper LN, Clementz MT, Usip S, Bajpai S, Hussain ST, Hieronymus TL (2016) Aquatic habits of cetacean ancestors: integrating bone microanatomy and stable isotopes. Integr Comp Biol 56:1370–1384. https://doi.org/10.1093/icb/icw119

Currey JD (2013) Bones: Structure and Mechanics. Princeton University Press, Princeton. https://doi.org/10.1515/9781400849505

D'Août K, Vereecke EE, Schoonaert K, De Clercq D, Van Elsacker L, Aerts P (2004) Locomotion in bonobos (*Pan paniscus*): differences and similarities between bipedal and quadrupedal terrestrial walking, and a comparison with other locomotor modes. J Anat 204:353–361. https://doi.org/10.1111/j.0021-8782.2004.00292.x

Debuysschere M (2015) Origine et première diversification des mammaliaformes : apport des faunes du Trias supérieur de Lorraine, France. Dissertation, Muséum national d'Histoire naturelle, Paris Desmond AJ (1975) The Hot-Blooded Dinosaurs. Blond and Briggs, London

Didier G, Laurin M (2020) Exact distribution of divergence times from fossil ages and tree topologies. Syst Biol 69:1068–1087. https://doi.org/10.1093/sysbio/syaa021

Doube M, Klosowski MM, Arganda-Carreras I, Cordelières FP, Dougherty RP, Jackson JS, Schmid B, Hutchinson JR, Shefelbine SJ (2010) BoneJ: free and extensible bone image analysis in ImageJ. Bone 47:1076–1079. https://doi.org/10.1016/j.bone.2010.08.023

Everitt BS, Skrondal A (2010) The Cambridge Dictionary of Statistics. Cambridge University Press, Cambridge

Fabbri M, Navalón G, Benson RBJ, Pol D, O'Connor J, Bhullar BAS, Erickson GM, Norell MA, Orkney A, Lamanna MC, Zouhri S, Becker J, Emke A, Dal Sasso C, Bindellini G, Maganuco S, Auditore M, Ibrahim N (2022) Subaqueous foraging among carnivorous dinosaurs. Nature 603:1–6. https://doi.org/10.1038/s41586-022-04528-0

Gambaryan PP, Kielan-Jaworowska Z (1997) Sprawling versus parasagittal stance in multituberculate mammals. Acta Palaeontol Pol 42:13–44

Gambaryan PP, Kuznetsov AN (2013) An evolutionary perspective on the walking gait of the long-beaked echidna. J Zool 290:58–67. https://doi.org/10.1111/jzo.12014

Gatesy SM (1991) Hind limb movements of the American alligator (*Alligator mississippiensis*) and postural grades. J Zool 224:577–588. https://doi.org/10.1111/j.1469-7998.1991.tb03786.x

Gatesy SM, Biewener AA (1991) Bipedal locomotion: effects of speed, size and limb posture in birds and humans. J Zool 224:127–147. https://doi.org/10.1111/j.1469-7998.1991.tb04794.x

Gerkema MP, Davies WI, Foster RG, Menaker M, Hut RA (2013) The nocturnal bottleneck and the evolution of activity patterns in mammals. Proc R Soc Lond B Biol Sci 280:20130508. https://doi.org/10.1098/rspb.2013.0508

Germain D, Laurin M (2005) Microanatomy of the radius and lifestyle in amniotes (Vertebrata, Tetrapoda). Zool Scr 34:335–350. https://doi.org/10.1111/j.1463-6409.2005.00198.x

Gill PG, Purnell MA, Crumpton N, Brown KR, Gostling NJ, Stampanoni M, Rayfield EJ (2014) Dietary specializations and diversity in feeding ecology of the earliest stem mammals. Nature 512:303–305. https://doi.org/10.1038/nature13622

675 Girondot M, Laurin M (2003) Bone Profiler: a tool to quantify, model, and statistically compare
676 bone-section compactness profiles. J Vertebr Paleontol 23:458–461

677 Gônet J, Laurin M, Girondot M (2022) BoneProfileR: the next step to quantify, model and
678 statistically compare bone section compactness profiles. Palaeontol Electron 25:a12
679 https://doi.org/10.26879/1194

680 Gregory WK (1912) Notes on the principles of quadrupedal locomotion and on the mechanism
681 of the limbs in hoofed animals. Ann N Y Acad Sci 22:267–294.
682 https://doi.org/10.1111/j.1749-6632.1912.tb55164.x

683 Hastie T, Tibshirani R, Buja A (1994) Flexible discriminant analysis by optimal scoring. J Am
684 Stat Assoc 89:1255–1270. https://doi.org/10.1080/01621459.1994.10476866

685 Hopson JA (2015) Fossils, trackways, and transitions in locomotion: a case study of
686 *Dimetrodon*. In: Dial KP, Shubin N, Brainerd EL (eds) Great Transformations in
687 Vertebrate Evolution. University of Chicago Press, Chicago, pp 125–141

688 Horovitz I, Ladevèze S, Argot C, Macrini TE, Martin T, Hooker JJ, Kurz C, Muizon C de,
689 Sánchez-Villagra MR (2008) The anatomy of *Herpetotherium* cf. *fugax* Cope, 1873, a
690 metatherian from the Oligocene of North America. Palaeontographica Abt A 284:109–
691 141. https://doi.org/10.1127/pala/284/2008/109

692 Houssaye A, Botton-Divet L (2018) From land to water: evolutionary changes in long bone
693 microanatomy of otters (Mammalia: Mustelidae). Biol J Linn Soc Lond 125:240–249.
694 https://doi.org/10.1093/biolinnean/bly118

695 Houssaye A, Sander PM, Klein N (2016a) Adaptive patterns in aquatic amniote bone
696 microanatomy—more complex than previously thought. Integr Comp Biol 56:1349–
697 1369. https://doi.org/10.1093/icb/icw120

698 Houssaye A, Waskow K, Hayashi S, Cornette R, Lee AH, Hutchinson JR (2016b)
699 Biomechanical evolution of solid bones in large animals: a microanatomical
700 investigation. Biol J Linn Soc Lond 117:350–371. https://doi.org/10.1111/bij.12660

701 Houssaye A, Taverne M, Cornette R (2018) 3D quantitative comparative analysis of long bone
702 diaphysis variations in microanatomy and cross-sectional geometry. J Anat 232:836–
703 849. https://doi.org/10.1111/joa.12783

Hu Y, Meng J, Wang Y, Li C (2005) Large Mesozoic mammals fed on young dinosaurs. Nature 433:149–152. https://doi.org/10.1038/nature03102

Hunt AP, Lucas SG (1998) Vertebrate tracks and the myth of the belly-dragging, tail-dragging tetrapods of the Late Paleozoic. N M Mus Nat Hist Bull 12:67–69

Hutchinson JR (2006) The evolution of locomotion in archosaurs. C R Palevol 5:519–530. https://doi.org/10.1016/j.crpv.2005.09.002

Hutchinson JR (2021) The evolutionary biomechanics of locomotor function in giant land animals. J Exp Biol 224:jeb217463. https://doi.org/10.1242/jeb.217463

Ibrahim N, Sereno PC, Dal Sasso C, Maganuco S, Fabbri M, Martill DM, Zouhri S, Myhrvold NP, Iurino DA (2014) Semiaquatic adaptations in a giant predatory dinosaur. Science 345:1613–1616. https://doi.org/10.1126/science.1258750

Isler K (2005) 3D-kinematics of vertical climbing in hominoids. Am J Phys Anthropol 126:6681. https://doi.org/10.1002/ajpa.10419

Jenkins FA (1971) Limb posture and locomotion in the Virginia opossum (*Didelphis marsupialis*) and in other non-cursorial mammals. J Zool 165:303–315. https://doi.org/10.1111/j.1469-7998.1971.tb02189.x

Jenkins FA (1973) The functional anatomy and evolution of the mammalian humero-ulnar articulation. Am J Anat 137:281–297. https://doi.org/10.1002/aja.1001370304

Jenkins FA, Parrington FR (1976) The postcranial skeletons of the Triassic mammals *Eozostrodon*, *Megazostrodon* and *Erythrotherium*. Philos Trans R Soc Lond B Biol Sci 273:387–431. https://doi.org/10.1098/rstb.1976.0022

Jenkins FA, Weijs WA (1979) The functional anatomy of the shoulder in the Virginia opossum (*Didelphis virginiana*). J Zool 188:379–410. https://doi.org/10.1111/j.1469-7998.1979.tb03423.x

Jones KE, Dickson BV, Angielczyk KD, Pierce SE (2021) Adaptive landscapes challenge the "lateral-to-sagittal" paradigm for mammalian vertebral evolution. Curr Biol 31:18831892. https://doi.org/10.1016/j.cub.2021.02.009

Kemp TS (2005) The Origin and Evolution of Mammals. Oxford University Press, Oxford. https://doi.org/10.1093/oso/9780198507604.001.0001

733 Kielan-Jaworowska Z, Hurum JH (2006) Limb posture in early mammals: sprawling or
734 parasagittal. Acta Palaeontol Pol 51:393–406

735 Kielan-Jaworowska Z, Cifelli RL, Luo Z-X (2004) Mammals from the Age of Dinosaurs:
736 Origins, Evolution, and Structure. Columbia University Press, New York

737 Kilbourne B, Hutchinson JR (2019) Morphological diversification of biomechanical traits:
738 mustelid locomotor specializations and the macroevolution of long bone cross-sectional
739 morphology. BMC Evol Biol 19:37. https://doi.org/10.1186/s12862-019-1349-8

740 Klein N, Sander PM, Krahl A, Scheyer TM, Houssaye A (2016) Diverse aquatic adaptations in
741 *Nothosaurus* spp. (Sauropterygia)—inferences from humeral histology and
742 microanatomy. PLoS One 11:e0158448. https://doi.org/10.1371/journal.pone. 0158448

743 Kriloff A, Germain D, Canoville A, Vincent P, Sache M, Laurin M (2008) Evolution of bone
744 microanatomy of the tetrapod tibia and its use in palaeobiological inference. J Evol Biol
745 21:807–826. https://doi.org/10.1111/j.1420-9101.2008.01512.x

746 Kurz C (2005) Ecomorphology of opossum-like marsupials from the Tertiary of Europe and a
747 comparison with selected taxa. Kaupia 14:21–26

748 Laurin M, Canoville A, Germain D (2011) Bone microanatomy and lifestyle: a descriptive
749 approach. C R Palevol 10:381–402. https://doi.org/10.1016/j.crpv.2011.02.003

750 Lebrun R (2018) MorphoDig, an open-source 3D freeware dedicated to biology. IPC5 Abstract
751 Book:399

752 Lin Y-F, Konow N, Dumont ER (2019) How moles walk; it's all thumbs. Biol Lett
753 15:20190503. https://doi.org/10.1098/rsbl.2019.0503

754 Main RP, Simons EL, Lee AH (2021) Interpreting mechanical function in extant and fossil long
755 bones. In: de Buffrénil V, de Ricqlès AJ, Zylberberg L, Padian K, Laurin M, Quilhac A
756 (eds) Vertebrate Skeletal Histology and Paleohistology. CRC Press, Boca Raton, pp
757 688–723

758 Meier PS, Bickelmann C, Scheyer TM, Koyabu D, Sánchez-Villagra MR (2013) Evolution of
759 bone compactness in extant and extinct moles (Talpidae): exploring humeral
760 microstructure in small fossorial mammals. BMC Evol Biol 13:110.
761 https://doi.org/10.1186/1471-2148-13-55

762 Meng J (2014) Mesozoic mammals of China: implications for phylogeny and early evolution
763 of mammals. Natl Sci Rev 1:521542. https://doi.org/10.1093/nsr/nwu070

764 Motani R, Schmitz L (2011) Phylogenetic versus functional signals in the evolution of form–
765 function relationships in terrestrial vision. Evolution 65:2245–2257.
766 https://doi.org/10.1111/j.1558-5646.2011.01271.x

767 Myhrvold NP, Baldridge E, Chan B, Sivam D, Freeman DL, Ernest SKM (2015) An amniote
768 life-history database to perform comparative analyses with birds, mammals, and
769 reptiles. Ecology 96:3109–3109. https://doi.org/10.1890/15-0846R.1

770 Nakajima Y, Hirayama R, Endo H (2014) Turtle humeral microanatomy and its relationship to
771 lifestyle. Biol J Linn Soc Lond 112:719–734. https://doi.org/10.1111/bij.12336

772 Niemitz C (2010) The evolution of the upright posture and gait—a review and a new synthesis.
773 Naturwissenschaften 97:241–263. https://doi.org/10.1007/s00114-009-0637-3

774 Pagel M (1999) Inferring the historical patterns of biological evolution.

775 Nature 401:877–884. https://doi.org/10.1038/44766

776 Parrish JM (1987) The origin of crocodilian locomotion. Paleobiology 13:396–414.
777 https://doi.org/10.1017/S0094837300009003

778 Pietersen DW, Jansen R, Swart J, Panaino W, Kotze A, Rankin P, Nebe B (2020) Temminck's
779 pangolin *Smutsia temminckii* (Smuts, 1832). In: Challender DWS, Nash HC, Waterman
780 C (eds) Pangolins: Science, Society and Conservation. Elsevier, Amsterdam, pp 175–
781 193. https://doi.org/10.1016/B978-0-12-815507-3.00011-3

782 Pinheiro J, Bates D, DebRoy S, Sarkar D, R Core Team (2021) nlme: linear and nonlinear
783 mixed effects. R package version 3.1–153

784 Plasse M, Amson E, Bardin J, Grimal Q, Germain D (2019) Trabecular architecture in the
785 humeral metaphyses of non-avian reptiles (Crocodylia, Squamata and Testudines):
786 lifestyle, allometry and phylogeny. J Morphol 280:982–998.
787 https://doi.org/10.1002/jmor.20996

788 Preuschoft H, Witte H, Christian A, Fischer M (1996) Size influences on primate locomotion
789 and body shape, with special emphasis on the locomotion of 'small mammals'. Folia
790 Primatol 66:93112. https://doi.org/10.1159/000157188

791 Pridmore PA (1985) Terrestrial locomotion in monotremes (Mammalia: Monotremata). J Zool
792 205:53–73. https://doi.org/10.1111/j.1469-7998.1985.tb05613.x

793 Quemeneur S, de Buffrénil V, Laurin M (2013) Microanatomy of the amniote femur and
794 inference of lifestyle in limbed vertebrates. Biol J Linn Soc Lond 109:644–655.
795 https://doi.org/10.1111/bij.12066

796 R Core Team (2013) R: a language and environment for statistical computing. R Foundation
797 for Statistical Computing, Vienna

798 Regnault S, Fahn-Lai P, Norris RM, Pierce SE (2020) Shoulder muscle architecture in the
799 echidna (Monotremata: *Tachyglossus aculeatus*) indicates conserved functional
800 properties. J Mamm Evol 27:591–603. https://doi.org/10.1007/s10914-020-09498-6

801 Reilly SM, Elias JA (1998) Locomotion in *Alligator mississippiensis*: kinematic effects of
802 speed and posture and their relevance to the sprawling-to-erect paradigm. J Exp Biol
803 201:2559–2574. https://doi.org/10.1242/jeb.201.18.2559

804 Revell LJ (2012) phytools: an R package for phylogenetic comparative biology (and other
805 things). Methods Ecol Evol 3:217–223. https://doi.org/10.1111/j.2041-
806 210X.2011.00169.x

807 Rose KD (2006) The Beginning of the Age of Mammals. Johns Hopkins University Press,
808 Baltimore

809 Rose JA, Sandefur M, Huskey S, Demler JL, Butcher MT (2013) Muscle architecture and out-
810 force potential of the thoracic limb in the eastern mole (*Scalopus aquaticus*). J Morphol
811 274:1277–1287. https://doi.org/10.1002/jmor.20178

812 Russo GA, Kirk EC (2017) Another look at the foramen magnum in bipedal mammals. J Hum
813 Evol 105:24–40. https://doi.org/10.1016/j.jhevol.2017.01.018

814 Scheidt A, Wölfer J, Nyakatura JA (2019) The evolution of femoral cross-sectional properties
815 in sciuromorph rodents: influence of body mass and locomotor ecology. J Morphol
816 280:11561169. https://doi.org/10.1002/jmor.21007

817 Seilacher A (1970) Arbeitskonzept zur Konstruktions-Morphologie. Lethaia 3:393–396.
818 https://doi.org/10.1111/j.1502-3931.1970.tb00830.x

819 Selva C (2017) Morphologie et fonction du système vestibulaire de l'oreille interne des
820 mammifères souterrains. Dissertation, Muséum national d'Histoire naturelle, Paris

821 Sereno PC (2006) Shoulder girdle and forelimb in multituberculates: evolution of parasagittal
822 forelimb posture in mammals. In: Carrano MT, Gaudin TJ, Blob RW, Wible JR (eds)
823 Amniote Paleobiology: Perspectives on the Evolution of Mammals, Birds, and Reptiles.
824 University of Chicago Press, Chicago, pp 315–366

825 Shannon CE (1948) A mathematical theory of communication. Bell Sys Tech J 27:379–423.
826 https://doi.org/10.1002/j.1538-7305.1948.tb01338.x

827 Shimer HW (1903) Adaptations to aquatic, arboreal, fossorial and cursorial habits in mammals.
828 III. Fossorial adaptations. Am Nat 37:819–825. https://doi.org/10.1086/278368

829 Stadler T (2011) Mammalian phylogeny reveals recent diversification rate shifts. Proc Natl
830 Acad Sci U S A 108:6187–6192. https://doi.org/10.1073/pnas.1016876108

831 Stein BR, Casinos A (1997) What is a cursorial mammal? J Zool 242:185–192.
832 https://doi.org/10.1111/j.1469-7998.1997.tb02939.x

833 Stone M (1974) Cross-validatory choice and assessment of statistical predictions. J R Stat Soc
834 Series B Stat Methodol 36:111133. https://doi.org/10.1111/j.2517-
835 6161.1974.tb00994.x

836 Tommasini SM, Nasser P, Schaffler MB, Jepsen KJ (2005) Relationship between bone
837 morphology and bone quality in male tibias: implications for stress fracture risk. J Bone
838 Miner Res 20:1372–1380. https://doi.org/10.1359/JBMR.050326

839 Upham NS, Esselstyn JA, Jetz W (2019) Inferring the mammal tree: species-level sets of
840 phylogenies for questions in ecology, evolution, and conservation. PLoS Biol
841 17:e3000494. https://doi.org/10.1371/journal.pbio.3000494

842 Vaughan TA, Ryan JM, Czaplewski NJ (2015) Mammalogy. Jones and Bartlett Learning,
843 Burlington

844 Wagstaffe AY, O'Driscoll AM, Kunz CJ, Rayfield EJ, Janis CM (2022) Divergent locomotor
845 evolution in "giant" kangaroos: evidence from foot bone bending resistances and
846 microanatomy. J Morphol 283:313–332. https://doi.org/10.1002/jmor.21445

847 Wilson GP, Evans AR, Corfe IJ, Smits PD, Fortelius M, Jernvall J (2012) Adaptive radiation
848 of multituberculate mammals before the extinction of dinosaurs. Nature 483:457–460.
849 https://doi.org/10.1038/nature10880

850 Wright M (2018) Functional morphology of the hindlimb during the transition from sprawling
851 to parasagittal gaits in synapsid evolution. Dissertation, Harvard University and
852 University of Groningen